ASN NEURO RESEARCH ARTICLE commentary multi-media ASN NEURO 1(5):art:e00022.doi:10.1042/AN20090040

# Dynamic imaging of cannabinoid receptor 1 vesicular trafficking in cultured astrocytes

**Kyle D Osborne*[1], William Lee[†1], Erik B Malarkey[†,‡], Andrew J Irving[§] and Vladimir Parpura[†2]**
*Department of Biological Sciences, Mt. San Antonio College, Walnut, CA 91789, U.S.A.
[†]Department of Neurobiology, Atomic Force Microscopy and Nanotechnology Laboratories, Center for Glial Biology in Medicine, Civitan International Research Center, Evelyn F. McKnight Brain Institute, University of Alabama, Birmingham, AL 35294, U.S.A.
[‡]Department of Pharmacology, School of Medicine, University of Washington, Seattle, WA 98195, U.S.A.
[§]Neurosciences Institute, Division of Medical Sciences, Ninewells Hospital and Medical School, University of Dundee, Dundee DD1 9SY, U.K.

**Cite this article as:** Osborne KD, Lee W, Malarkey EB, Irving AJ and Parpura V (2009) Dynamic imaging of cannabinoid receptor 1 vesicular trafficking in cultured astrocytes. ASN NEURO 1(5):art:e00022.doi:10.1042/AN20090040

## ABSTRACT

Astrocytes possess GPCRs (G-protein-coupled receptors) for neuroactive substances and can respond via these receptors to signals originating from neurons as well as astrocytes. Like many transmembrane proteins, GPCRs exist in a dynamic equilibrium between receptors expressed at the plasma membrane and those present within intracellular trafficking compartments. The characteristics of GPCR trafficking within astrocytes have not been investigated. We therefore monitored the trafficking of recombinant fluorescent protein chimeras of the CB1R (cannabinoid receptor 1) that is thought to be expressed natively in astrocytes. CB1R chimeras displayed a marked punctate intracellular localization when expressed in cultured rat visual cortex astrocytes, an expression pattern reminiscent of native CB1R expression in these cells. Based upon trafficking characteristics, we found the existence of two populations of vesicular CB1R puncta: (i) relatively immobile puncta with movement characteristic of diffusion and (ii) mobile puncta with movement characteristic of active transport along cytoskeletal elements. The predominant direction of active transport is oriented radially to/from the nuclear region, which can be abolished by disruption of the microtubule cytoskeleton. CB1R puncta are localized within intracellular acidic organelles, mainly co-localizing with endocytic compartments. Constitutive trafficking of CB1R to and from the plasma membrane is an energetically costly endeavour whose function is at present unclear in astrocytes. However, given that intracellular CB1Rs can engage cell signalling pathways, it is likely that this process plays an important regulatory role.

Key words: actin, acutely isolated astrocyte, cannabinoid receptor, microtubule, vesicular trafficking.

## INTRODUCTION

Astrocytes are a diverse population of glial cells, with functions ranging from structural support to modulation of synaptic transmission. Astrocytes possess a multitude of receptors [reviewed in (Verkhratsky, 2006)] for signalling molecules released by neurons and themselves, including the cannabinoid receptor 1, CB1R (Rodriguez et al., 2001), which is thought to mediate neuron–astrocyte communication (Navarrete and Araque, 2008). Protein trafficking plays an important role in regulating CB1R expression, with receptors changing localization between the plasma membrane and intracellular compartments. In certain cell types at rest, CB1R is constitutively endocytosed, leading to a predominantly intracellular localization (Leterrier et al., 2004; McDonald et al., 2007a). Thus endocytic trafficking can be an important regulator of CB1R availability at the plasma membrane.

Few studies on protein trafficking have been carried out in astrocytes. These have been limited to studies of the secreted ANP (atrial natriuetic peptide), the serpin PN-1 (protease nexin-1) and the synaptic-vesicle-associated protein synaptobrevin

[1] Both of these authors contributed equally to this work.
[2] To whom correspondence should be addressed (email vlad@uab.edu).
**Abbreviations:** ANP, atrial natriuetic peptide; CB1R, cannabinoid receptor 1; DIC, differential interference contrast; EYFP, enhanced yellow fluorescent protein; GFAP, glial fibrillary acidic protein; GFP, green fluorescent protein; GPCR, G-protein-coupled receptor; HBSS, Hanks balanced salt solution; LSD, least significant difference; α-MEM, α-minimum essential medium; MSD, mean square displacement; NA, numerical aperture; P1 etc., postnatal day 1 etc; PEI, polyethyleneimine; PN-1, protease nexin-1; RT–PCR, reverse transcription–PCR; SEP, superecliptic pHluorin; TRITC, tetramethylrhodamine β-isothiocyanate; VAMP8, vesicle-associated membrane protein 8; V-ATPase, vacuolar-type proton ATPase.

2 (Giau et al., 2005; Potokar et al., 2005; Crippa et al., 2006; Potokar et al., 2007). As these molecules all function within the exocytotic pathway, they are likely to have similar trafficking dynamics and may be found within common vesicle pools. As the picture of how proteins found within the exocytotic pathway traffic in astrocytes is being elucidated, there are no comparative data as to the trafficking of receptors, such as GPCRs (G-protein-coupled receptors), in astrocytes. The trafficking of GPCRs, such as CB1R and the β-2 adrenergic receptor, which are expressed by astrocytes (Aoki et al., 1987; Rodriguez et al., 2001), is better understood in other cell types, particularly with regard to endocytic trafficking (Coutts et al., 2001; Leterrier et al., 2004; Shumay et al., 2004).

In the present study, we have investigated CB1R expression and intracellular trafficking within cultured astrocytes isolated from rat visual cortex. Fluorescent CB1R chimeras were used in combination with pharmacological agents to examine CB1R trafficking dynamics. Our findings indicate that within cultured astrocytes at rest there is a pronounced vesicular pool of CB1Rs, which is trafficked both by microtubule- and actin-based mechanisms; microtubule-dependent radial shuttling towards and away from the cell centre is evident. In addition, a population of CB1R–GFP (green fluorescent protein) was found to be relatively immobile, with movement characteristic of passive diffusion. Astrocytes expressing a SEP (superecliptic pHluorin)-tagged CB1R (SEP–CB1R) and treated with bafilomycin A1 showed the presence of CB1R within low-pH endocytic intracellular compartments. We found that the punctate CB1R–GFP label mainly co-localized with the endosomal marker endobrevin [also referred to as VAMP8 (vesicle-associated membrane protein 8)].

Trafficking of receptors to and from the astrocyte plasma membrane probably shapes astrocytic responses to signalling molecules, but the nature of receptor trafficking in astrocytes has yet to be investigated in detail. To our knowledge the present study of CB1R trafficking constitutes the first investigation of receptor protein trafficking in astrocytes. This should be of additional importance when one considers the previous demonstration of preferential localization of CB1R *in situ* to the astrocytic end-foot (Rodriguez et al., 2001). Future studies of CB1R trafficking in more intact systems may help to develop our understanding of how membrane proteins are preferentially localized to distinct domains of astrocytes and how they influence local cell signalling.

## MATERIALS AND METHODS

### Cell culture

All animal procedures were in strict accordance with the National Institutes of Health Guide for Care and Use of Laboratory Animals and were approved by the University of Alabama at Birmingham Institutional Animal Care and Use Committee.

Visual cortices were dissected from 0–2-day-old Sprague–Dawley rats and treated with papain (20 i.u./ml; Sigma) in HBSS (Hanks balanced salt solution; Invitrogen) for 1 h at 37°C. The tissue was washed with HBSS and then incubated with trypsin inhibitor (type II-O, 10 mg/ml; Sigma) in HBSS for 5 min. After an additional wash with HBSS, the tissue was triturated in culture medium containing α-MEM (α-minimum essential medium; Invitrogen) supplemented with 10% FBS (fetal bovine serum; Hyclone), 20 mM glucose, 2 mM L-glutamine, 1 mM sodium pyruvate, 14 mM sodium bicarbonate, 100 i.u./ml penicillin and 100 μg/ml streptomycin (pH 7.35). The resulting cell suspension was applied to culture flasks and maintained in culture medium at 37°C in a 5% $CO_2$/95% air incubator. After 6–15 days, the cells were submitted to a procedure for purification of astrocytes. At that time, flasks were shaken on a horizontal orbital shaker at 260 rev./min for 1.5 h, and after changing the medium twice, shaken again for 18 h. The cells that remained attached to the bottom of the flask were then returned to the incubator to be submitted to the transfection protocol (see below) or plated on coverslips as follows. Prior to experiments, cells were detached using trypsin [10000 BAEE (*N*α-benzoyl-L-arginine ethyl ester hydrochloride) units/ml; Sigma–Aldrich] in HBSS and then pelleted using centrifugation at 100 ***g*** for 10 min. The resulting cell pellet was resuspended in complete medium and plated on to glass coverslips (12 mm in diameter) pre-coated with 1 mg/ml PEI (polyethyleneimine). The cells were used in experiments after 2–10 days. This culture method yields >99% astrocytes (Montana et al., 2004).

### RT–PCR (reverse transcription-PCR)

Total RNA was extracted from purified cultures of astrocytes from visual cortex and from whole-brain tissue of postnatal Sprague–Dawley rats (0–2-days-old) using TRIzol® reagent (Invitrogen) according to the manufacturer's protocol. Total RNA (5 μg) was used for reverse transcription using oligo$(dT)_{12-18}$ and superscript II reverse transcriptase (Invitrogen). Primers for CB1R (GenBank® accession number U40395) amplification were 5′-CCTTCAGGGG-TAGTCCCTTC-3′ and 5′-ACATTGGGGCTGTCTTTACG-3′ (producing a 412 bp product).

### Cell transfection

Transfection was performed using purified astrocytic culture and a transfection reagent (TransIT-293; Mirus). At 1 h prior to the transfection procedure, the astrocyte culture medium was completely exchanged for fresh medium. The transfection agent was prepared by mixing α-MEM with no additives and TransIT-293 (36 μl/flask) reagent, followed by vortex-mixing and incubating for 10 min at room temperature (20–24°C). At this time, plasmid DNA (6 μg/flask) was added to the mixture and incubated for 10 min at room

temperature. The mixture was evenly dispersed into dishes containing astrocytes grown on PEI-coated coverslips, which were incubated for 1 h at 37°C in a 5% $CO_2$/95% air incubator. Following incubation and wash-out of transfection mixture, fresh complete medium was applied and cells were returned to the incubator for 48–96 h, at which time they were used for experiments. The following plasmids encoding CB1R–GFP variant chimeras were used for the present study. (i) The full-length CB1R with the enhanced GFP fused to the C-terminus (CB1R–GFP). To generate C-terminally tagged CB1R–GFP, rat CB1R (wild-type) was introduced into the pEGFP-N1 plasmid (Clontech) between Hind3 and BamHI cloning sites. The integrity of the construct was confirmed by DNA sequencing. (ii) The full-length CB1R N-terminally tagged with GFP or SEP and a signal sequence from human growth hormone, in a pcDNA1 vector (GFP–CB1R and SEP–CB1R respectively) (McDonald et al., 2007b). (iii) GFP–CB1R truncated at its C-terminus and lacking 14 amino acids (GFP–CB1RΔ14). The plasmid encoding the light chain of clathrin tagged with DsRed (a red fluorescent protein; in the pDsRed-N1 vector, Clontech) at the C-terminus, CLC–DsRed, was kindly provided by Wolfhard Almers (Oregon Health and Science University, Portland, OR, U.S.A.) (Merrifield et al., 2002). Additional plasmids encoding fluorescent protein-tagged cytoskeletal proteins were: (i) DsRed appended to the C-terminus of the β5-tubulin, tubulin–DsRed, kindly provided by Vincent Homburger (Institut de Genomique Fonctionnelle, Montpellier, France) (Giau et al., 2005); and (ii) EYFP (enhanced yellow fluorescent protein) fused to the N-terminus of the human β-actin, EYFP–actin (Clontech).

## Indirect immunocytochemistry

Cultured astrocytes were fixed with 4% (w/v) paraformaldehyde in PBS (pH=7.4) for 30 min at room temperature. Cells were then permeabilized using 0.25% Triton X-100 for 10 min. PBS supplemented with 10% goat serum was used to block non-specific binding and cells were then incubated with the primary antibody overnight at 4°C. Rabbit polyclonal antibodies against CB1R (2 μg/ml; Frontier Science) and endobrevin/VAMP8 (1:250; Synaptic Systems), as well as the monoclonal mouse antibody against synaptobrevin 2 (1:250 dilution; catalogue number 104 201, Synaptic Systems; please note that this product has been replaced by the manufacturer with catalogue number 104 211), were used. Following washing, cells were incubated with TRITC (tetramethylrhodamine isothiocyanate)-conjugated secondary antibody for 1 h. Coverslips were then washed and mounted on to glass slides with 1% n-propyl gallate for image acquisition.

## Acutely isolated astrocytes

Cells were acutely isolated from visual cortices of 1- and 8-day-old Sprague–Dawley rats using a modification (Montana et al., 2004) of a previously described procedure (Zhou and Kimelberg, 2000). Briefly, visual cortices isolated from rats were subjected to papain treatment, followed by a trituration as described for cell cultures. After trituration, cells were applied to PEI-coated coverslips and allowed to adhere for 1 h. After washing, cells were fixed for immunocytochemistry. We co-labelled acutely isolated astrocytes using the rabbit antibody against CB1R and the mouse monoclonal antibody against the astrocytic marker GFAP (glial fibrillary acidic protein; 1:500; MP Biomedicals). Following overnight incubation with primary antibodies at 4°C, washed cells were incubated with FITC (fluorescein isothiocyanate) (for GFAP)- and TRITC (for CB1R)-conjugated secondary antibodies for 1 h, washed and mounted on to glass slides with 1% n-propyl gallate for image acquisition. Positive staining for CB1R and GFAP was defined by the average pixel intensity across the entire cell that was at least three S.D.s above background fluorescence of cells in which CB1R/GFAP primary antibody were omitted. All imaging data were background corrected by subtracting the fluorescence emission from a coverslip region containing no cells.

## Imaging acquisition and processing

All experiments were performed at room temperature. For live-cell imaging, cells were bathed in an external solution that contained 140 mM NaCl, 5 mM KCl, 2 mM $CaCl_2$, 2 mM $MgCl_2$, 5 mM glucose and 10 mM Hepes (pH=7.4). We used an inverted microscope (TE 300; Nikon) equipped with DIC (differential interference contrast) and wide-field epifluorescence illumination. Visualization of indirect immunocytochemistry was accomplished using a standard rhodamine/TRITC filter set (excitation 535 nm/emission 610 nm) and a fluorescein/FITC filter set (excitation 480 nm/emission 535 nm). A standard fluorescein/FITC filter set was used for visualization of CB1R–GFP chimeras and EYFP–actin. A standard Texas Red filter set (excitation 560 nm/emission 630 nm) was utilized for visualization of CLC–DsRed and tubulin–DsRed. All filter sets were from Chroma Technology. Images were captured through a 60× plan-Apo oil-immersion objective [numerical aperture (NA), 1.4; Nikon] using a CoolSNAP-HQ cooled CCD (charged-coupled device) camera (Roper Scientific) driven by V++ imaging software (Digital Optics) or MetaMorph Software (Molecular Devices). For time-lapse image acquisition, a camera and an electronic shutter (Vincent Associates) inserted into the excitation pathway were controlled by imaging software. A Xenon arc lamp (100 W) was used as a light source. All images shown in the Figures and Movie 1 represent raw data with their pixel intensities within the dynamic range (0–4095) of the camera (CoolSNAP-HQ).

## $Ca^{2+}$ imaging

Intracellular $Ca^{2+}$ levels in astrocytes were monitored using the $Ca^{2+}$ indicator fluo-3 (Parpura et al., 1994; Parpura and Haydon, 2000). Briefly, cells were loaded at room temperature in external solution, containing fluo-3 AM (where AM is

acetoxymethyl ester, 10 μg/ml; Invitrogen) and Pluronic acid (0.025%; Invitrogen) for 30 min. After washing in external solution, the $Ca^{2+}$ indicator was permitted to de-esterify for 30 min at room temperature in external solution. Coverslips containing dye-loaded cells were mounted on to a recording chamber and imaged with a 20× plan-Fluor air objective (0.5 NA; Nikon) or a 60× plan-Apo oil-immersion objective. A FITC filter set was used to visualize fluo-3 fluorescence. Data were background subtracted using a fluorescence image acquired in a region of coverslip without cells. Fluo-3 intensity changes of entire astrocytes were expressed as d*F*/*F*o (%), where d*F* represents the change of fluorescence after cell stimulation and *F*o represents the average fluorescence (11 consecutive images) of the cell before stimulation. Stimulation of astrocytes with the CB1R agonist WIN55,212-2 (1–10 μM, 80 s) was achieved by its delivery via a puffer pipette connected to the PicoSpritzer II pressure ejection system (~70 kPa; Parker Haniffin). To assess the proper loading of the $Ca^{2+}$ indicator, at the end of each experiment, cells were incubated with the $Ca^{2+}$ ionophore 4-bromo-A23187 (10 μM, 3 min; Invitrogen). For further analysis we only considered cells that displayed an increase in d*F*/*F*o>100% after incubation with the ionophore. Astrocytes were considered responsive to the agonist if d*F*/*F*o values were higher than *F*o+3S.D.s in at least two consecutive images.

## CB1R tracking

Tracking of CB1R fluorescent puncta was performed using MetaMorph software to acquire 60 frames, 1.5 frame/s time-lapse series. The 200 highest-intensity puncta that were between 4 and 70 pixels [the width of one pixel corresponds to 106 nm, imposed by the calculated Rayleigh's transverse resolution of 233 nm (at 535 nm emission) and by the Nyquist–Shannon sampling theorem] in area were selected for trafficking analysis. Only puncta found in thin regions of astrocytes, peripheral to the perinuclear region, were tracked to minimize the artefact associated with movement in the *z*-axis as previously described (Potokar et al., 2005). Additionally, the puncta that could not be tracked through the entire time-lapse series, and those that intersected each other, were discarded. Data were exported to Excel (Microsoft) and algorithms were used to determine the instantaneous velocity, maximal displacement (distance between the furthest two points along a path of a punctum), total track length and directionality index (ratio of maximal displacement to total track length) for each punctum, as previously described (Potokar et al., 2005). A custom-written Visual Basic routine for Excel, referred to in the present study as a custom script, was used to determine the movement of puncta relative to the nucleus and plot the track of each punctum.

## Pharmacological agents

Agents used in the assessment of intracellular $Ca^{2+}$ levels are described above in the section on $Ca^{2+}$ imaging. All drugs used in trafficking experiments to affect microtubule or actin cytoskeleton dynamics were incubated with the cells prior to imaging and were maintained in the external solution during the imaging procedure. Colchicine (1 μM; 45 min) was used for the disassembly of microtubules, whereas latrunculin B (5 μM; 45 min) was used to cause disassembly of F-actin. To stabilize the microtubule cytoskeleton, paclitaxel (taxol) (1 μM; 1 h) was used, whereas jasplakinolide (1 μM; 1 h) was used to stabilize F-actin. Bafilomycin A1 (5 μM; 30 min) was incubated with cells to block V-ATPase (vacuolar-type proton ATPase). All agents were from Sigma–Aldrich, except latrunculin B and jasplakinolide (EMD Biosciences).

## Statistical analysis

The effect of WIN55,212-2 on astrocytic intracellular $Ca^{2+}$ levels and changes in SEP–CB1R fluorescence due to application of bafilomycin A1 or its vehicle (0.1% DMSO in external solution) were assessed using a paired *t* test. A Student's *t* test was used to assess the difference in instantaneous velocity of directional and non-directional puncta, as well as to test any differences in instantaneous velocity of directional puncta moving towards/away from the nucleus. The comparison between trafficking measurements using N- and C-terminally labelled CB1R and the effect of C-terminal truncation on trafficking was also tested using a Student's *t* test. The effect of pharmacological agents affecting the actin and microtubule cytoskeletons was tested using one-way ANOVA followed by Fisher's LSD (least significant difference) test. The averages of each trafficking measurement were made for all puncta of individual cells, and the compiled cell averages for each experimental group were tested. All results are expressed as means±S.E.M. To determine whether displacement angles were normally distributed, a D'Agostino test was used. The dip test (Hartigan, 1985; Hartigan and Hartigan, 1985) was done to test for unimodality of displacement angle distributions using the R 2.8.1 program with dip-test package installed (The R Foundation for Statistical Computing).

# RESULTS

## Expression of native CB1R in visual cortex astrocytes

Previous reports have questioned the presence of CB1R in cultured astrocytes, whereas their expression *in situ* has been more accepted [for a review see (Stella, 2004)]. Visual cortex astrocytes have not been investigated for the presence of CB1R up to this point. Thus, in the present study, we probed purified visual cortex astrocyte cultures for the expression of CB1R using a combination of immunocytochemistry, RT–PCR analysis and $Ca^{2+}$ imaging (Figure 1). Indeed, mRNA for the

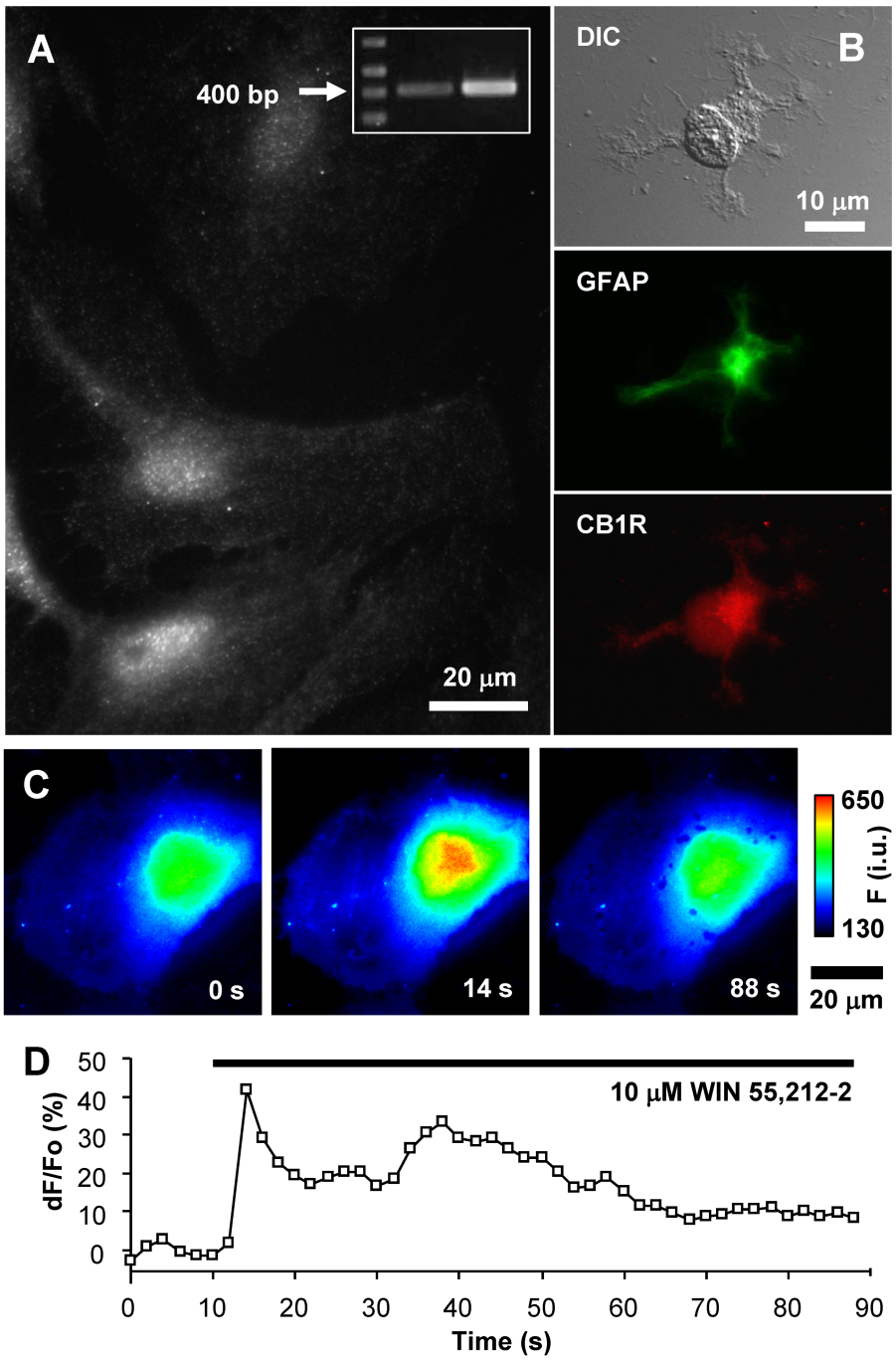


**Figure 1** **Expression of CB1R in visual cortex astrocytes**
**(A)** Localization of CB1R in cultured rat visual cortex astrocytes was identified by indirect immunocytochemistry using an antibody against CB1R. Astrocytes display puncate staining throughout the entire cell body with some accumulation in the perinuclear region. RT–PCR identified the presence of CB1R mRNA in cultured astrocytes (inset). The arrow indicates the 400 bp marker. RT–PCR primers were designed to amplify a 412 bp fragment of the full-length CB1R transcript (middle lane, astrocytes; right-hand lane, whole brain). **(B)** Indirect immunocytochemistry using antibodies against GFAP and CB1R on acutely isolated astrocytes from visual cortex of P1 rats. Acutely isolated astrocytes that were identified by the presence of the specific marker GFAP (green, FITC) show typical stellate morphology (DIC) and CB1R (red, TRITC) stain reminiscent of that seen in cultured astrocytes. **(C)** Stimulation of an astrocyte with the CB1R agonist WIN55,212-2 (10 μM) causes an increase in the internal $Ca^{2+}$ elevations. The pseudocolour scale is a linear representation of the fluorescence intensities ranging from 130 to 650 intensity units (i.u.). Times (in s) indicated on images correspond to the time on the *x*-axis of the graph displaying a time-lapse of fluo-3 fluorescence, reporting on internal $Ca^{2+}$ levels. **(D)** Changes in fluo-3 fluorescence are shown as d*F*/*Fo* (%) after background subtraction. The horizontal bar in the graph indicates the application of WIN55,212-2.

CB1R was detected in these cells (Figure 1A, inset). Immunocytochemical labelling of CB1R with a CB1R antibody raised against a previously characterized epitope (Katona et al., 2006; Uchigashima et al., 2007) revealed that cultured astrocytes have CB1Rs present throughout the cell, with some accumulation in the perinuclear region, and show a punctate staining pattern (Figure 1A). Since the expression of CB1R in cultured astrocytes may result from gene expression changes with culturing (Wilhelm et al., 2004), and not reflect expression within the brain, we tested whether CB1R is expressed in acutely isolated astrocytes from visual cortex by immunocytochemistry. Astrocytes acutely isolated in this manner have been shown to retain much of the gene expression profile of those *in situ* (Kimelberg et al., 2000a, 2000b; Montana et al., 2004; Malarkey et al., 2008). Using animals at postnatal days (P) 1 and 8, we found the expression of CB1R in 52% (24 out of 46 tested) and 69% (9 out of 14 tested) of acutely isolated astrocytes respectively; staining was similar to that found in cultured astrocytes (Figure 1B). To test functionality of CB1R in cultured astrocytes we used $Ca^{2+}$ imaging, since CB1R activation has been demonstrated to cause $Ca^{2+}$ excitability in hippocampal astrocytes (Navarrete and Araque, 2008). Consistent with that finding, application of the CB1R agonist WIN55,212-2 (1–10 μM, 80 s) to astrocytes from visual cortex caused an increase in intracellular $Ca^{2+}$ levels (Figures 1C and 1D) in all cells tested (3 out of 3 at 1 μM; and 11 out of 11 at 10 μM; peak response $dF/Fo = 111 \pm 18\%$; paired $t$ test, $P < 0.01$). Taken together these experiments demonstrate functional CB1R expression within visual cortex astrocytes.

## Mobility of CB1R–GFP in cultured astrocytes

In order to monitor the trafficking dynamics of CB1R we transfected cultured astrocytes with a plasmid encoding CB1R–GFP. Astrocytes expressing CB1R–GFP displayed bright punctate fluorescence throughout the cell, with some accumulation in the perinuclear region (Figure 2A and Movie 1) reminiscent of native CB1R expression (Figure 1A). Puncta 4–70 pixels large were tracked to investigate CB1R mobility. The distribution of puncta sizes within the 4–70 pixel range for a single cell is shown in Figure 2(B). A similar distribution pattern was observed with all cells. Examples of paths taken for tracked puncta are shown in Figure 2(C), coded in time by colour, and the position of the nucleus is denoted by the large open circle. For the tracking of CB1R–GFP puncta, we defined a greater than 1 μm maximum displacement as directional mobility. A distance of 1 μm approximates 1% of the diameter of a cultured astrocyte (Potokar et al., 2005), and, within the time elapsed (40 s) in our trafficking experiments, it is a distance that cannot be attained by simple diffusion of an 80 nm particle in

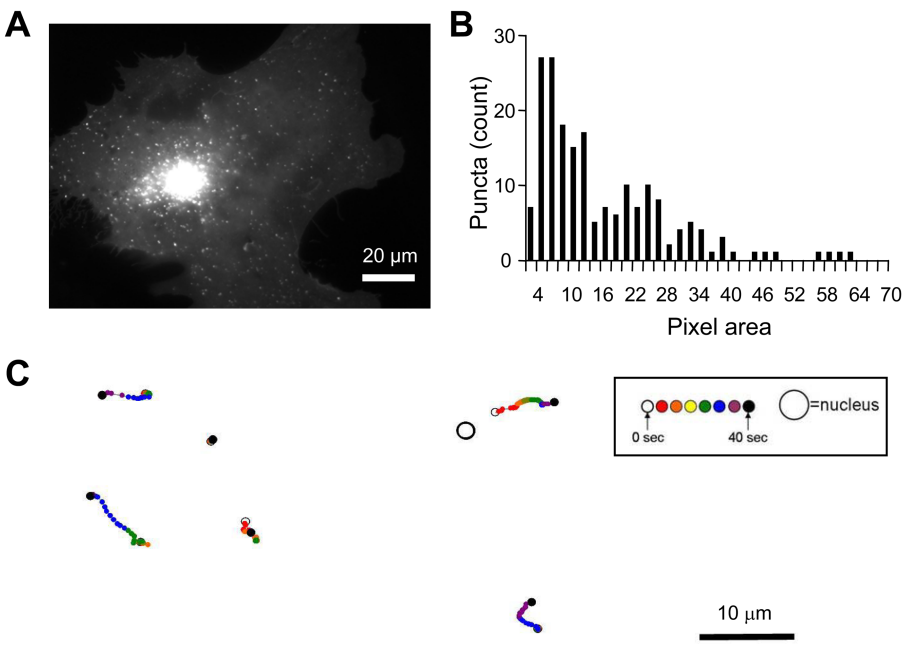


**Figure 2** **Expression and trafficking of CB1R–GFP in astrocytes**
(**A**) Astrocyte expressing full-length CB1R appended by GFP at its C-terminus (CB1R–GFP). The fluorescence pattern is similar to that of native CB1R with puncta present throughout entire cell, with some accumulation within the perinuclear region of the cell. (**B**) Distribution of CB1R–GFP puncta sizes within the size range selected for trafficking analysis for a single cell. For measurements of CB1R–GFP trafficking, 200 puncta ranging from 4 to 70 pixels (one pixel is equal to 106 nm × 106 nm) in area were selected based on pixel intensity. Most of the puncta tracked fall within the 4–20 pixel area, whereas the incidence of puncta greater than 50 pixels in area was minor. (**C**) Example paths of tracked CB1R–GFP puncta coded in time by colour. The relative position of the travelled path of each punctum is indicated by the position of the nucleus (not drawn to scale). Both long-distance and short-range tracks can be observed. The time-lapse sequence of the intracellular CB1R–GFP trafficking in astrocyte in (**A**) is shown in Movie 1.

cytoplasm (Luby-Phelps, 2000), which is approximately the size of trafficking vesicles identified in astrocytes (Crippa et al., 2006). The majority of CB1R–GFP puncta were found to fall within the non-directional category, having maximum displacement values less than 1 μm (Figure 3A). In comparing non-directional to directional puncta, it was found that non-directional puncta display instantaneous velocities significantly lower than that of puncta within the directional category (Figure 3B; Student's *t* test, $P<0.01$). By plotting MSD (mean square displacement) as a function of time, a linear relationship was found for non-directional puncta (Figure 3C) which can be fitted ($r^2 = 0.996$) by eqn (1):

$$\text{MSD}\ (\mu\text{m}^2) = 0.064\ \mu\text{m}^2/\text{s} \times \text{time}\ (\text{s}) + 0.0114\ \mu\text{m}^2 \qquad (1)$$

This is consistent with the movement of non-directional puncta being governed by simple diffusion, where the slope in the above equation can be used to calculate an apparent diffusion coefficient (D) of $1.6 \times 10^{-10}$ $\text{cm}^2/\text{s}$ using eqn (2):

$$\text{MSD} = 4\text{Dt} \qquad (2)$$

[For a detailed procedure see (Potokar et al., 2005).] The movement of directional puncta appears to be governed by a more complex mechanism(s) than simple diffusion and it can be best fitted by a power relationship ($r^2 = 0.999$), followed by a dual reciprocal function ($r^2 = 0.980$).

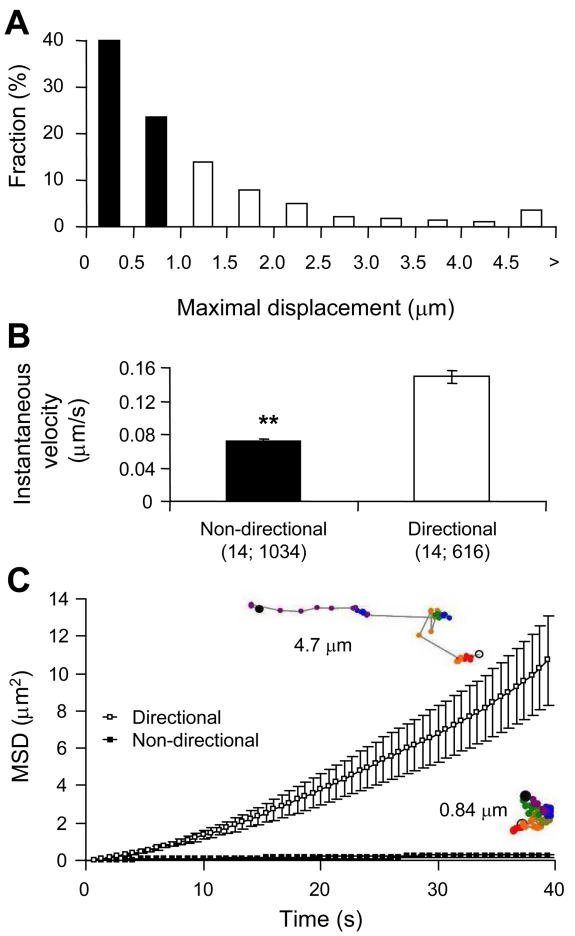


**Figure 3 Mobility of CB1R–GFP puncta in astrocytes**
(**A**) CB1R–GFP puncta were tracked during a 60 frame time-lapse series (40 s; Movie 1) and categorized by their maximal displacement, with non-directional puncta having maximal displacement less than 1 μm (solid bars) and directional greater than 1 μm (open bars). The histogram shows the relative frequency of maximal displacement values, expressed as a percentage for all puncta ($n=1650$) within the cell analysed ($n=14$). (**B**) Non-directional CB1R–GFP puncta (solid bar) display a significantly slower instantaneous velocity compared with the directional group (open bar) (Student's *t* test, $^{**}P<0.01$). Bars represent mean instantaneous velocity ± S.E.M. Values in parentheses indicate the number of cells; total number of puncta. (**C**) Graph showing the average MSD ± S.E.M. as a function of time for all tracked CB1R–GFP puncta within the non-directional (■) and directional (□) categories. Examples of single puncta mobility tracks for each category are shown next to the graph traces and are colour-coded for time as described in Figure 2(C); the total track length is 4.7 μm and 0.84 μm for directional and non-directional puncta respectively.

## Role of distal C-terminus in CB1R trafficking dynamics

The C-terminus of transmembrane proteins such as GPCRs often has an important role in the trafficking of the receptor. The distal C-terminus of CB1R has previously been implicated in endocytosis of the receptor (Hsieh et al., 1999) and may also bind CRIP (cannabinoid receptor interacting protein) 1a (Niehaus et al., 2007). To test whether the C-terminus has a role in the trafficking dynamics of CB1R, an N-terminally GFP-tagged CB1R with a C-terminal 14-amino-acid truncation (Δ14aa) was expressed in cultured astrocytes. We determined instantaneous velocity, maximal displacement, the fraction of directional puncta (having a greater than 1 μm maximal displacement), total track length and directionality index of GFP-tagged CB1R puncta. The directionality index was used to determine the extent of rectilinear movement. Comparing measurements of trafficking dynamics for cells expressing GFP–CB1RΔ14aa to the control/full-length GFP–CB1R we found that the absence of the C-terminal 14 amino acids resulted in a significant reduction in a subset of trafficking parameters (instantaneous velocity and total track length; Student's *t* test, $P<0.05$) (Figures 4A and 4D; column 1 compared with column 2). When we compared trafficking dynamics for cells expressing the N-terminally tagged GFP–CB1R to C-terminally tagged CB1R–GFP, however, we found that tagging CB1R at its C-terminus had no significant effect on any parameter tested (Student's *t* test; $P=0.08$–$0.97$ for various parameters; Figures 4A–4E; column 2 compared with column 3). Taken together these findings may reflect a specific function of the distal part of the CB1R C-terminus in receptor trafficking, but will require further studies of regulatory protein interactions within this region to support this idea.

## Role of actin and microtubule cytoskeletons in CB1R–GFP trafficking

We investigated the role of cytoskeletal elements on the trafficking of CB1R with the use of pharmacological agents

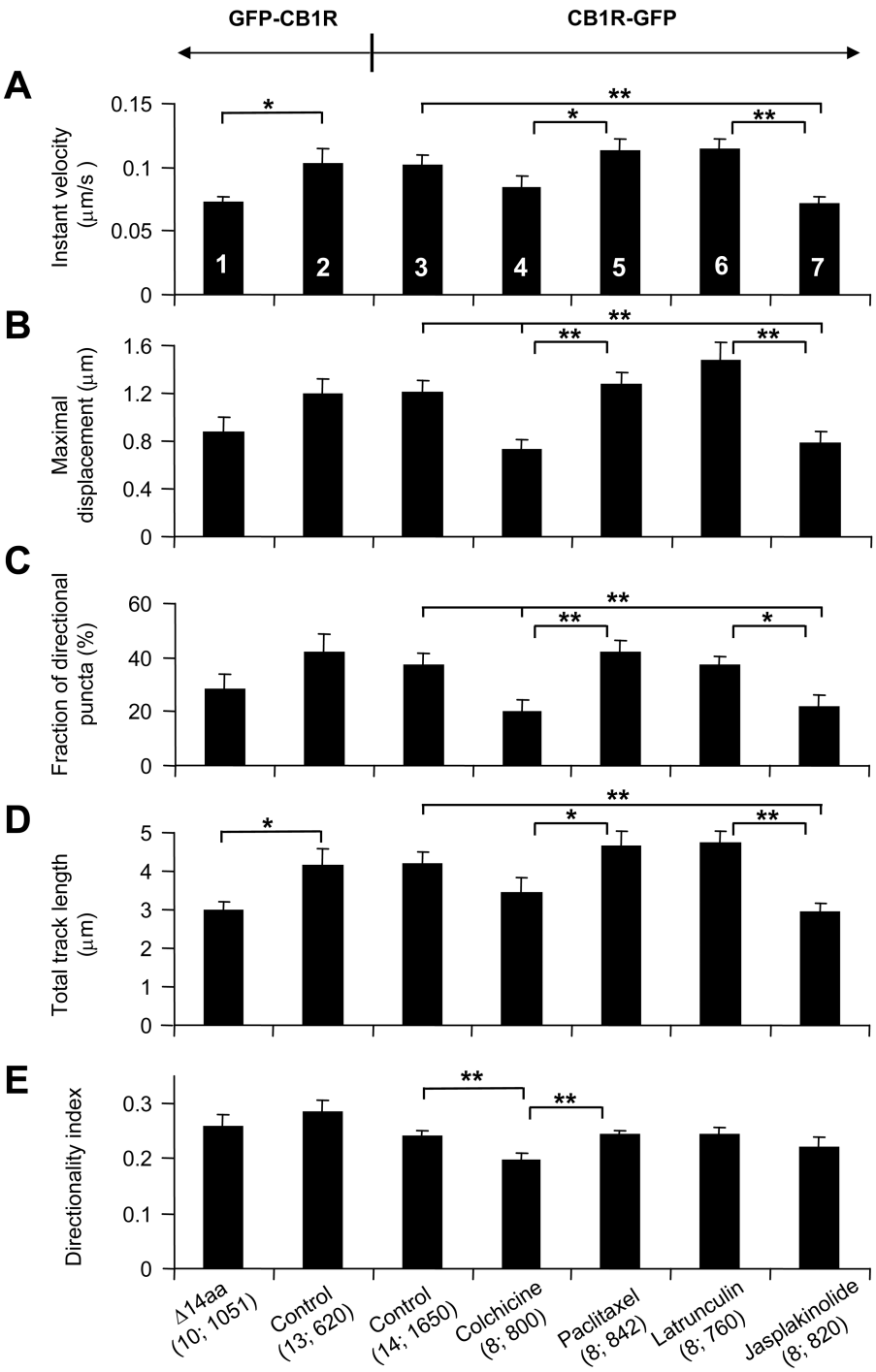


**Figure 4** **Distal C-terminal truncation of CB1R affects intracellular trafficking of this receptor, which utilizes microtubules and actin filaments for its traffic**

(**A**–**E**) Trafficking dynamics for cells expressing N-terminally tagged GFP–CB1R (column 2) display similar characteristics (no statistical difference) as C-terminally tagged CB1R–GFP (column 3). Truncation of GFP–CB1R at its C-terminal 14 amino acids (Δ14aa) reduces the instantaneous (Instant) velocity (**A**) and total track length (**D**) when compared with the control cells expressing the full-length GFP–CB1R (compare columns 1 and 2; Student's *t* test, $^*P<0.05$). (**A**) Instantaneous velocity analysis of C-terminally tagged CB1R–GFP shows a decrease from control (column 3) when cells are treated with jasplakinolide (column 7). (**B**) Average maximal displacement was reduced significantly compared with control when cells were treated with colchicine and jasplakinolide (compare columns 3, 4 and 7). (**C**) The fraction of directional puncta was reduced when cells were treated with colchicine and jasplakinolide (compare columns 3, 4 and 7). (**D**) The average total length of tracks travelled by puncta was shorter for jasplakinolide-treated cells (compare columns 3 and 7). (**E**) The directionality index was reduced compared with control when cells were treated

with colchicine (compare columns 3 and 4). Treatments with opposing actions on microtubules, disruption by colchicine and stabilization by paclitaxel, show a significant difference in all measured parameters (compare columns 4 and 5). Similarly, treatments with opposing actions on actin meshwork, disruption by latrunculin B and stabilization by jasplakinolide, show a significant difference in all measured parameters (**A–D**; compare columns 6 and 7), with the exception of the directionality index (**E**). The effect of pharmacological agents affecting cytoskeletal elements on C-terminally labelled CB1R–GFP trafficking was statistically tested using one-way ANOVA followed by a post-hoc Fisher's LSD test; *$P<0.05$ and **$P<0.01$ respectively. All bars, numbered by column to aid comparison, represent means ± S.E.M. of individual cell averages for tracked puncta. Values in parentheses indicate number of cells; total number of puncta.

to either disrupt or stabilize microtubule and actin cytoskeleton dynamics. The effect of cytoskeleton-disrupting agents, colchicine for destabilization of microtubule and latrunculin B for destabilization of actin filaments, was verified using astrocytes expressing tubulin–DsRed or EYFP–actin respectively. We found that the fluorescence intensities of microtubule tracks, as visualized by tubulin–DsRed, and actin filaments, as visualized by EYFP–actin, were reduced after treatment with these cytoskeleton-disrupting agents (data not shown). To assess the role of cytoskeletal elements in CB1R trafficking, astrocytes expressing CB1R–GFP were subjected to incubation with pharmacological agents prior to acquiring time-lapse series. Trafficking measurements for drug-treated cells were compared with control untreated cells, to determine the dependence on microtubules or actin filaments in CB1R–GFP trafficking (Figure 4; columns 3–7). All parameters except instantaneous velocity and total track length were decreased when astrocytes were treated with colchicine to depolymerize microtubules (Figures 4B, 4C and 4E; column 3 compared with column 4; one-way ANOVA followed by Fisher's LSD test, $P<0.01$). The effect of colchicine on reducing the directionality index implicates microtubule-based transport in long-distance, straight-line movement of CB1R–GFP. When microtubules were stabilized using paclitaxel, no difference from control was observed, but a significant increase in all parameters was seen when compared with colchicine-treated cells (Figures 4A–4E; column 4 compared with column 5, one-way ANOVA followed by Fisher's LSD test, $P<0.05$ or $P<0.01$ for various parameters). Actin depolymerization with latrunculin B had no significant effect on trafficking parameters from controls (Figure 4; column 3 compared with column 6), but it showed significantly greater trafficking parameters, with the exception of directionality index, when compared with astrocytes treated with jasplakinolide to cause actin filament stabilization (Figures 4A–4D; column 6 compared with column 7; one-way ANOVA followed by Fisher's LSD test, $P<0.05$ or $P<0.01$ for various parameters). Astrocytes treated with jasplakinolide resulted in a significant decrease in all measurements, with the exception of directionality index, when compared with control (Figures 4A–4D; column 3 compared with column 7, one-way ANOVA followed by Fisher's LSD test, $P<0.01$), indicating that an interaction with actin filaments may act to slow CB1R–GFP puncta velocity. Taken together, these data show that both microtubules and actin filaments play a role in CB1R–GFP trafficking in astrocytes.

## Preferential radial trafficking of directional CB1R–GFP puncta along microtubules

Since pharmacological experiments suggest that much of the directional trafficking of CB1R–GFP relies on microtubule-based mechanisms, we attempted to verify movement along microtubules visually. When CB1R–GFP was co-expressed in astrocytes with tubulin–DsRed, which labelled microtubules with red fluorescent protein, CB1R–GFP puncta could be seen travelling along the track of microtubules (data not shown). The dynamics of puncta seen moving along microtubules travelled at higher rates, consistent with microtubule-based trafficking, further suggesting microtubule-based mechanisms for the trafficking. Therefore a strategy was devised in an attempt to find any pattern or preferential movement of directional puncta. Since across cell types microtubules polymerize in a radial manner from the microtubule-organizing centre to the cell periphery, and our results suggest that directional CB1R trafficking relies on microtubules, we investigated whether there was a preference for radially patterned movement. A custom script was written to plot the path of each directional punctum (maximal displacement values greater than 1 μm) relative to the nucleus in which trajectory displacement angles away from the nucleus were assigned positive angles ranging from 0 to 90° with increasing angles more tangential, whereas those towards the nucleus were assigned by the same convention with negative angles (Figure 5A). We first assessed whether directional puncta moving towards or away from the nucleus showed differences in trafficking velocity. No difference in the instantaneous velocity was found between structures trafficking towards or away from the nucleus (Figure 5B; $n=13$, Student's $t$ test, $P=0.5$). To determine whether particular directions of active transport predominate, analysis was conducted using histograms of trajectory displacement angles for directional puncta ($n=557$ from 13 cells). Angles near 0° were found to predominate with a significantly unimodal distribution [dip test, $D(F_{557})=0.0106$, $P<0.05$], even though the normality of distribution was rejected (D'Agostino Test, $D'=3772.9$; $P<0.01$), indicating that the majority of CB1R–GFP puncta were trafficking more radially directly towards or away from the nucleus (Figure 5C).

Since microtubules are arranged in a radial pattern centred at the microtubule-organizing centre near the cell nucleus, it was suspected that transport along microtubules might underlie the observed preferential trafficking of directional CB1R–GFP. To test this we compared colchicine- and latrunculin-B-treated cells with untreated control cells

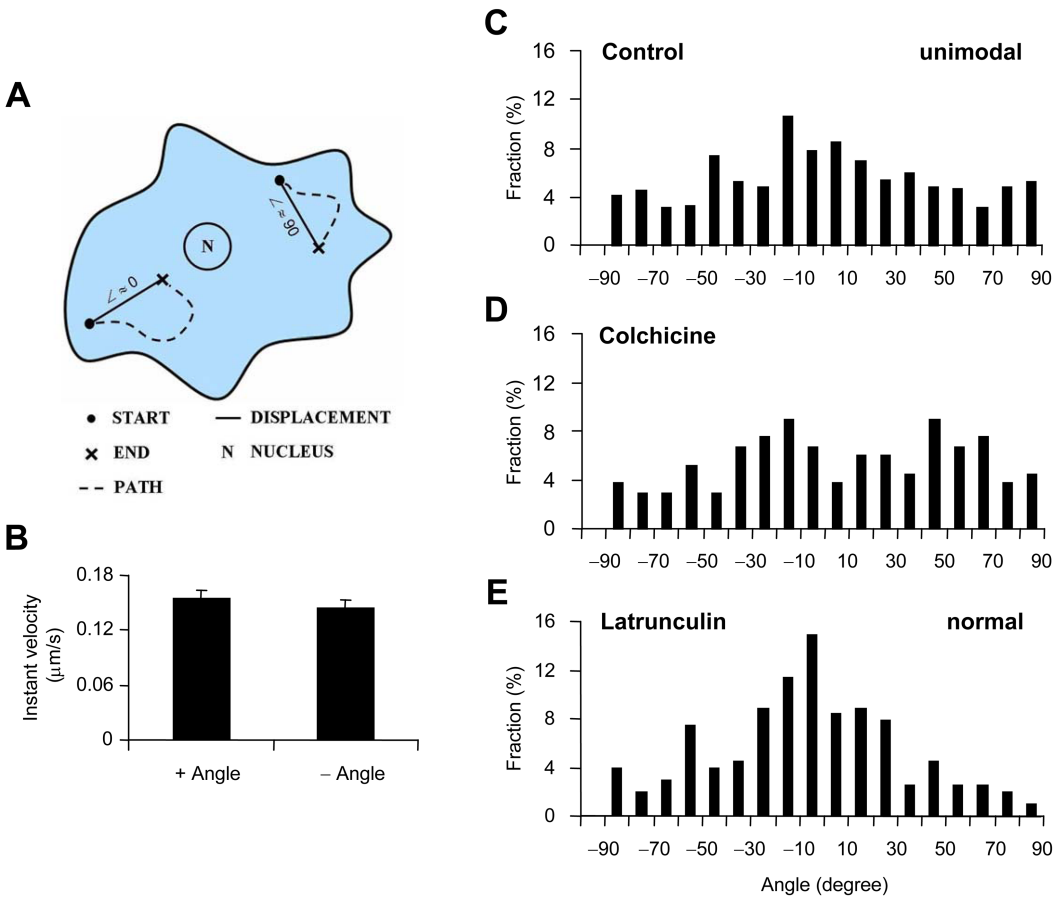


**Figure 5** **Preferential radial trafficking of directional CB1R–GFP**

(**A**) Diagram shows the convention used for defining displacement angles (∠), ranging from −90° to 90°, from the path (dotted line) of the individual directional CB1R–GFP puncta. Angle values approach 0° as trajectories become more radial, directly towards or away from the nucleus of the cell (N), whereas more tangential trajectories associate with angle values approaching ±90°. (**B**) The instantaneous (Instant) velocity of directional CB1R–GFP puncta trafficking away (+ Angle) from the nucleus was no different from that observed for puncta travelling towards (− Angle) the nucleus ($n$=13 cells). (**C–E**) Charts show frequency histograms of displacement angles for control (**C**), colchicine-treated (**D**) and latrunculin B-treated (**E**) cells . (**C**) Histogram of displacement angles for control cells shows unimodal distribution ($n$=557 puncta; dip-test, $P$<0.05) with the mode near 0° identifying the preferential mode of directional CB1R–GFP trafficking to be radial, towards and away from the nucleus, whereas a substantial amount of trafficking occurs tangential to the nucleus. (**D**) When cells were treated with colchicine, the preference for radial trafficking is abolished ($n$=133 puncta), with display of an apparent bimodal distribution. (**E**) Near 0° angles predominate with displacement angles showing normal ($n$=202 puncta; D'Agostino Test, $P$>0.05), albeit not unimodal, distribution, when astrocytes were treated with latrunculin B.

expressing CB1R–GFP. Depolymerization of microtubules with colchicine abolished the unimodal pattern [dip test, $D(F_{133})$=0.0319, $P$>0.05], whereas the normality of distribution remained rejected (D'Agostino Test, $D'$=441.3; $P$<0.01), confirming that radial traffic of directional CB1R–GFP puncta occured along microtubules. An apparent bimodal distribution arises with the angle trajectories near −20° and 50°, consistent with the remaining movement along actin filaments ($n$=133 from seven cells; Figure 5D). Treatment with latrunculin B to disrupt actin filaments accentuated the near 0° angles mode with a reduction in the frequency of larger angles (Figure 5E), indicating actin filament function in the trafficking of CB1R–GFP along tracks tangential to the nucleus. The distribution was not found to be unimodal [dip test, $D(F_{202})$=0.0213, $P$>0.05], but it was found normal (D'Agostino test, $D'$=809.7, $P$>0.05; $n$=202 from five cells). Taken together, it appears that the disruption of microtubules leads to the reduction of the preferential radial traffic based on the analysis of angle trajectories of directional CB1R–GFP puncta, which is consistent with the decrease of directionality index in colchicine-treated astrocytes (Figure 4E).

## Intracellular localization of CB1R in astrocytes

We used astrocytes expressing superecliptic pHluorin-tagged CB1R (SEP–CB1R; McDonald et al., 2007b), rather than GFP–CB1R, to initiate investigations into the subcellular localization of CB1R in astrocytes. Although GFP is pH-sensitive (Patterson et al., 1997), SEP has an enhanced pH sensitivity. Its fluorescence is nearly completely quenched at pH levels below 6 and quenching is relieved at higher pH (Miesenbock et al., 1998). Because the SEP is located on the

N-terminus of CB1R, which could be located in the acidic (pH<6) lumen of vesicular structures or extracellular fluid (pH=7.4) when on the plasma membrane, we can determine whether CB1R resides in acidic compartments. To this end we exposed cells expressing SEP–CB1R to bafilomycin A1, a blocker of V-ATPase, to cause de-acidification of low pH compartments (Figures 6A and 6B). With exposure to bafilomycin A1, cells expressing SEP–CB1R showed an increase in maximal fluorescence ($dF/Fo = 118 \pm 30\%$, $n=4$; paired $t$ test, $P<0.05$), which became highly punctate. However, in sham-treatment of cells where only the vehicle was applied, cells expressing SEP–CB1R did not show significant changes in maximal fluorescence ($dF/Fo = -22 \pm 8\%$, $n=5$; paired $t$ test, $P=0.14$). These results indicate that a population of CB1R resides in low pH intracellular compartments.

Since various cellular organelles have an acidic luminal pH established and maintained by V-ATPase, we additionally co-labelled astrocytes expressing CB1R–GFP with markers for various intracellular compartments to further study the

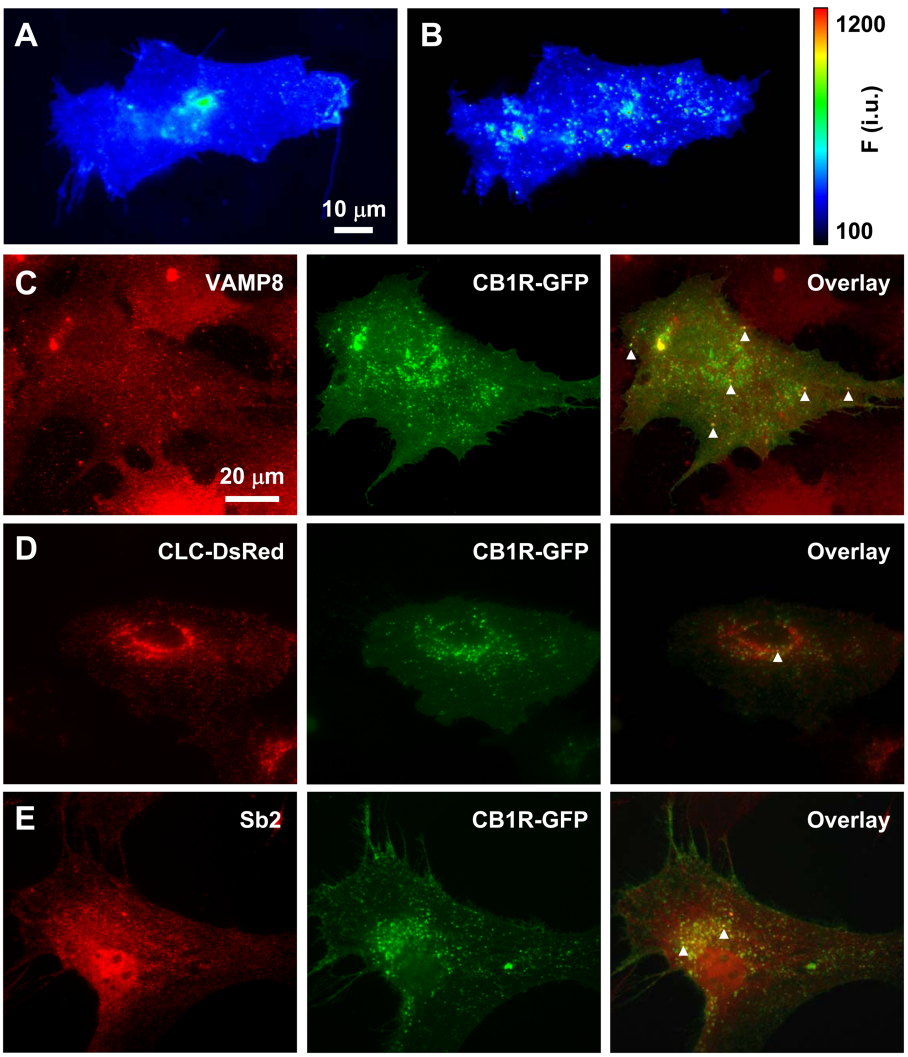


**Figure 6** **Intracellular CB1R localization in astrocytes**

(**A** and **B**) The presence of SEP–CB1R in low-pH intracellular structures. (**A**) Astrocyte expressing SEP–CB1R at rest. (**B**) After incubation with bafilomycin A1 to block V-ATPase, SEP–CB1R fluorescence intensity increases displaying more prominently punctate fluorescence indicating that a population of SEP–CB1R exists within acidic compartments. The pseudocolour scale is a linear representation of the fluorescence intensities ranging from 100 to 1200 intensity units (i.u.). (**C–E**) Intracellular CB1R–GFP localizes in endosomes. (**C**) CB1R–GFP (green, middle panel)-expressing astrocytes immunolabelled for endobrevin (VAMP8) (red, left-hand panel), an endosomal marker. Arrowheads mark some instances of co-localization of CB1R–GFP and endogenous VAMP8 (overlay, right-hand panel). (**D**) Co-expressed CLC–DsRed (red, left-hand panel), labelling early endocytic structures, and CB1R–GFP (green, middle panel) show very little co-localization (overlay, right-hand panel; arrowhead). (**E**) CB1R–GFP (green, middle panel)-expressing astrocytes immunolabelled for the exocytotic vesicle marker synaptobrevin 2 (Sb2) (red, left-hand panel). Subcellular localization of CB1R–GFP and Sb2 immunoreactivity show some overlap (overlay, right-hand panel; arrowheads) within the perinuclear region of the cell, whereas co-localization was not apparent at the periphery of the cell.

subcellular localization of this receptor. CB1R has been shown to be primarily endocytic in origin (Leterrier et al., 2004), and to undergo endocytosis through caveolae and clathrin-dependent pathways (Keren and Sarne, 2003). To test whether astrocytic CB1R is found within the endocytic pathway, we examined the co-localization of CB1R with endobrevin (VAMP8) (Figure 6C) and with clathrin (Figure 6D). Astrocytes expressing CB1R–GFP were either immunolabelled using an antibody against VAMP8 or they were co-transfected to co-express clathrin light-chain–DsRed (CLC–DsRed). CB1R–GFP mainly co-localized with VAMP8 immunoreactivity, whereas there was very little co-localization with CLC–DsRed. These results indicate the predominant localization of CB1R within endosomes containing VAMP8 over early endocytic structures containing clathrin. Moreover, astrocytes expressing CB1R–GFP were also immunolabelled using an antibody against the exocytotic protein synaptobrevin 2 (Figure 6E). CB1R–GFP co-localized with some of the synaptobrevin 2, which was evident in the perinuclear region of the cell, whereas peripheral co-localization was not detected.

## DISCUSSION

The presence of CB1R in cultured astrocytes has been found to vary between astrocyte cultures originating from different animal strains and between cultures originating from different brain areas (Stella, 2004). This may be explained by the emerging picture that astrocytes are a diverse population of cells that may have different gene-expression profiles dependent upon the particular region of the CNS (central nervous system) in which they reside. Using cultured rat visual cortex astrocytes we found CB1R to be expressed at the transcript and protein levels; these receptors are functional since their activation with a CB1R agonist leads to intracellular $Ca^{2+}$ excitability. In addition, we showed that CB1R is expressed in acutely isolated astrocytes of rat visual cortex, indicating that the expression of CB1R occurs in these astrocytes within the brain. Whether cultures of visual cortex astrocytes may therefore provide a suitable system to investigate the function of astrocytic CB1R as a distinct function of CB1R in astrocytes *in vivo* remains to be elucidated. Towards that end, there has been a recent demonstration that CB1R plays a role in neuron–astrocyte signalling in hippocampal slices (Navarrete and Araque, 2008).

The characteristics of protein trafficking in astrocytes have recently begun to be investigated, with particular emphasis on trafficking of proteins in the exocytotic pathway. The present study of CB1R trafficking in astrocytes constitutes the first investigation of protein trafficking dynamics of a plasma membrane expressed receptor in astrocytes. Under resting conditions, a large proportion of recombinant CB1R is constitutively endocytosed and present within intracellular vesicles in neurons (McDonald et al., 2007a) or HEK (human embryonic kidney)-293 cells (Leterrier et al., 2004). Since we observed a prominent perinuclear stain for native (Figures 1A and 1B) and exogenous (Figures 2A, and 6C–6E) CB1R, it is possible that this represents some of the recycled CB1R, in addition to its synthesis, suggesting that in visual cortex astrocytes the receptor could undergo marked constitutive endocytosis. We found, similarly to ANP (Potokar et al., 2005) and synaptobrevin 2 (Crippa et al., 2006), that the majority of CB1R puncta are immobile, as defined by maximum displacement values less than 1 μm. These results are in contrast with the finding that post-Golgi PN-1 vesicles are nearly all mobile (Giau et al., 2005). The fact that these authors selectively analysed vesicles that were newly budded from the Golgi network may account for some of the differences in the findings. To determine the underlying mechanism for movement of non-directional CB1R–GFP puncta, we examined the relationship between MSD and time. A linear relationship was found for non-directional puncta, indicating that diffusion may govern movement of puncta within this class. An apparent diffusion coefficient of $1.6 \times 10^{-10}$ $cm^2/s$ was calculated from the linear fit of MSD against time for non-directional puncta. The apparent diffusion coefficient for CB1R–GFP is less than that determined for ANP ($6.8 \times 10^{-10}$ $cm^2/s$) in astrocytes (Potokar et al., 2005). Overall it was observed that CB1R–GFP puncta trafficked at an instantaneous velocity of 0.11 μm/s, with directional puncta trafficking at an instantaneous velocity of 0.15 μm/s and non-directional puncta with an instantaneous velocity of 0.07 μm/s. In comparison with published data of velocities observed in astrocytes, CB1R–GFP-positive structures move at a slower rate. Velocities of 0.65 μm/s and 0.4 μm/s were found for synaptobrevin 2 (Crippa et al., 2006) and ANP (Potokar et al., 2005) respectively.

In general, movement at higher velocities, such as observed with directional CB1R puncta, is driven by motor proteins using microtubules or F-actin as tracks for directed movement (Evans and Bridgman, 1995; Goldstein and Yang, 2000). We therefore sought to determine the extent to which microtubules and/or actin filaments are used for the movement of CB1R. Through pharmacological disruption of these cytoskeletal elements we found CB1R–GFP trafficking to be dependent upon microtubules. In addition, an interaction was identified between CB1R–GFP puncta and actin filaments, as stabilization of actin filaments resulted in an overall decrease in CB1R–GFP mobility. Some evidence exists for actin-dependent trafficking within astrocytes (Stachelek et al., 2001); the hormone-activated trafficking of the enzyme type II deiodinase (D2) from the cell periphery to recycling endosomes is dependent upon myosin 5a, an actin-based motor protein. Although we found CB1R within the endocytic pathway in astrocytes and could therefore be trafficked to endosomes from the cell periphery similar to D2, our results suggest that this is not the case. Depolymerization of actin filaments resulted in no significant decrement of

trafficking measures for CB1R–GFP. If an actin-based transport were used for a component of CB1R trafficking, using perhaps myosin 5a, then depolymerizing actin filaments may reduce trafficking measures. Although it does not appear that long-range movement of CB1R occurs via actin-based mechanisms as observed with D2, since depolymerizing microtubules does not completely abolish active transport and since opposing pharmacological treatments to disrupt or stabilize actin caused significant differences in trafficking parameters, some actin-based trafficking of CB1R may occur. Cortical F-actin has been shown to regulate mobility of secretory granules and clathrin-mediated endocytosis, and, as such, it may be that the interaction of CB1R–GFP and actin is short-lived and occurs at the cell periphery (Lang et al., 2000; Merrifield et al., 2002). As would be expected by the arrangement of microtubules, we found directional CB1R–GFP puncta to preferentially traffic in a radial pattern from/to the nucleus. Cargo vesicles carrying CB1R–GFP to the cell periphery may, to some extent, underlie the radial traffic. Since it was found that a subpopulation of CB1R–GFP reside in endosomes, and long-range tracks toward the nucleus were observed, endosomal traffic may also constitute a portion of the radial trafficking of CB1R–GFP. Indeed there is evidence in the literature that could support a role for microtubules in CB1R endosomal trafficking. Leterrier et al. (2004) observed long-range movement of CB1R-positive endosomes. It should be noted that astrocytes express kinesins (Crippa et al., 2006). Energetically, transport of CB1R–GFP in astrocytes is costly, as microtubule-based motors and myosins expend one ATP molecule at each individual step. With a range of step-size for these motors from 8 to 30 nm (Howard et al., 1989; Rock et al., 2007), the ATP expense of the transport of a single CB1R–GFP punctum, at average instantaneous velocity, is between 5 and 19 ATP molecules used every second.

Classically, the relative amount of receptors expressed at the cell surface, which was beyond the scope of the present study, will shape the response to extrinsic signalling molecules. However, vesicular (intracellular) CB1Rs can still engage cell signalling (Gomes et al., 2009), which may be activated by lipophilic (membrane-permeant) cannabinoid ligands or via innate constitutive activity. Astrocytes play an active role in cell-to-cell communication in the brain, in part, reliant on neuroligand receptors. Investigations into the trafficking of receptors within astrocytes will provide important data as to astrocyte function. CB1R trafficking may be of particular interest within astrocytes; it was found that CB1R preferentially localizes to the astrocytic end-foot (Rodriguez et al., 2001). Preferential localization is governed by distinct sorting signals and pathways that effectively target proteins to their respective domain. Such signals and pathways governing targeting in astrocytes await identification. Astrocyte end-feet couple to each other along the vasculature through gap junctions formed by connexin 43 (Simard et al., 2003). Interestingly cannabinoid ligands have been demonstrated to block gap-junctional coupling in astrocytes, although CB1R was not directly implicated in this finding (Venance et al., 1995). Local signalling occurring at astrocyte end-feet can modulate cerebrovascular blood flow, and can spread via gap junctions along the vasculature (Simard et al., 2003; Mulligan and MacVicar, 2004). As the constitutive trafficking of CB1R to and from the plasma membrane is an energetically costly endeavour for astrocytes, this process is likely to play a role in shaping the cellular response to endogenous cannabinoid ligands or constitutive signalling activity. Thus future studies might investigate the involvement of cannabinoid signalling at the astrocyte end-foot, and the role of constitutive CB1R trafficking in this.

**ACKNOWLEDGEMENTS**

We dedicate this work to the late Glenn I. Hatton, whose energy and creativity inspired new views of astrocyte–neuronal interactions.

**FUNDING**

This work was supported by the National Institute of Mental Health [grant number MH 069791 (to V.P.)]; the National Science Foundation [grant number CBET 0943343 (to V.P.)]; TENOVUS Scotland (to A.J.I.); and the Anonymous Trust (to A.J.I.).

## REFERENCES

Aoki C, Joh TH, Pickel VM (1987) Ultrastructural localization of β-adrenergic receptor-like immunoreactivity in the cortex and neostriatum of rat brain. Brain Res 437:264–282.

Coutts AA, Anavi-Goffer S, Ross RA, MacEwan DJ, Mackie K, Pertwee RG, Irving AJ (2001) Agonist-induced internalization and trafficking of cannabinoid CB1 receptors in hippocampal neurons. J Neurosci 21:2425–2433.

Crippa D, Schenk U, Francolini M, Rosa P, Verderio C, Zonta M, Pozzan T, Matteoli M, Carmignoto G (2006) Synaptobrevin 2-expressing vesicles in rat astrocytes: insights into molecular characterization, dynamics and exocytosis. J Physiol 570:567–582.

Evans LL, Bridgman PC (1995) Particles move along actin filament bundles in nerve growth cones. Proc Natl Acad Sci USA 92:10954–10958.

Giau R, Carrette J, Bockaert J, Homburger V (2005) Constitutive secretion of protease nexin-1 by glial cells and its regulation by G-protein-coupled receptors. J Neurosci 25:8995–9004.

Goldstein LS, Yang Z (2000) Microtubule-based transport systems in neurons: the roles of kinesins and dyneins. Annu Rev Neurosci 23:39–71.

Gomes I, Grushko JS, Golebiewska U, Hoogendoorn S, Gupta A, Heimann AS, Ferro ES, Scarlata S, Fricker LD, Devi LA (2009) Novel endogenous peptide agonists of cannabinoid receptors. FASEB J 23:3020–3029.

Hartigan JA, Hartigan PM (1985) The dip test of unimodality. Anal Stat 13:70–84.

Hartigan PM (1985) Computation of the dip statistic to test for unimodality. Appl Stat 34:320–325.

Howard J, Hudspeth AJ, Vale RD (1989) Movement of microtubules by single kinesin molecules. Nature 342:154–158.

Hsieh C, Brown S, Derleth C, Mackie K (1999) Internalization and recycling of the CB1 cannabinoid receptor. J Neurochem 73:493–501.

Katona I, Urban GM, Wallace M, Ledent C, Jung KM, Piomelli D, Mackie K, Freund TF (2006) Molecular composition of the endocannabinoid system at glutamatergic synapses. J Neurosci 26:5628–5637.

Keren O, Sarne Y (2003) Multiple mechanisms of CB1 cannabinoid receptors regulation. Brain Res 980:197–205.

Kimelberg HK, Cai Z, Schools G, Zhou M (2000a) Acutely isolated astrocytes as models to probe astrocyte functions. Neurochem Int 36:359–367.

Kimelberg HK, Schools GP, Cai Z, Zhou M (2000b) Freshly isolated astrocyte (FIA) preparations: a useful single cell system for studying astrocyte properties. J Neurosci Res 61:577–587.
Lang T, Wacker I, Wunderlich I, Rohrbach A, Giese G, Soldati T, Almers W (2000) Role of actin cortex in the subplasmalemmal transport of secretory granules in PC-12 cells. Biophys J 78:2863–2877.
Leterrier C, Bonnard D, Carrel D, Rossier J, Lenkei Z (2004) Constitutive endocytic cycle of the CB1 cannabinoid receptor. J Biol Chem 279:36013–36021.
Luby-Phelps K (2000) Cytoarchitecture and physical properties of cytoplasm: volume, viscosity, diffusion, intracellular surface area. Int Rev Cytol 192:189–221.
Malarkey EB, Ni Y, Parpura V (2008) $Ca^{2+}$ entry through TRPC1 channels contributes to intracellular $Ca^{2+}$ dynamics and consequent glutamate release from rat astrocytes. Glia 56:821–835.
McDonald NA, Henstridge CM, Connolly CN, Irving AJ (2007a) An essential role for constitutive endocytosis, but not activity, in the axonal targeting of the CB1 cannabinoid receptor. Mol Pharmacol 71:976–984.
McDonald NA, Henstridge CM, Connolly CN, Irving AJ (2007b) Generation and functional characterization of fluorescent, N-terminally tagged CB1 receptor chimeras for live-cell imaging. Mol Cell Neurosci 35:237–248.
Merrifield CJ, Feldman ME, Wan L, Almers W (2002) Imaging actin and dynamin recruitment during invagination of single clathrin-coated pits. Nat Cell Biol 4:691–698.
Miesenbock G, De Angelis DA, Rothman JE (1998) Visualizing secretion and synaptic transmission with pH-sensitive green fluorescent proteins. Nature 394:192–195.
Montana V, Ni Y, Sunjara V, Hua X, Parpura V (2004) Vesicular glutamate transporter-dependent glutamate release from astrocytes. J Neurosci 24:2633–2642.
Mulligan SJ, MacVicar BA (2004) Calcium transients in astrocyte endfeet cause cerebrovascular constrictions. Nature 431:195–199.
Navarrete M, Araque A (2008) Endocannabinoids mediate neuron-astrocyte communication. Neuron 57:883–893.
Niehaus JL, Liu Y, Wallis KT, Egertova M, Bhartur SG, Mukhopadhyay S, Shi S, He H, Selley DE, Howlett AC, Elphick MR, Lewis DL (2007) CB1 cannabinoid receptor activity is modulated by the cannabinoid receptor interacting protein CRIP 1a. Mol Pharmacol 72:1557–1566.
Parpura V, Haydon PG (2000) Physiological astrocytic calcium levels stimulate glutamate release to modulate adjacent neurons. Proc Natl Acad Sci USA 97:8629–8634.
Parpura V, Basarsky TA, Liu F, Jeftinija K, Jeftinija S, Haydon PG (1994) Glutamate-mediated astrocyte-neuron signalling. Nature 369:744–747.
Patterson GH, Knobel SM, Sharif WD, Kain SR, Piston DW (1997) Use of the green fluorescent protein and its mutants in quantitative fluorescence microscopy. Biophys J 73:2782–2790.
Potokar M, Kreft M, Pangrsic T, Zorec R (2005) Vesicle mobility studied in cultured astrocytes. Biochem Biophys Res Commun 329:678–683.
Potokar M, Kreft M, Li L, Daniel Andersson J, Pangrsic T, Chowdhury HH, Pekny M, Zorec R (2007) Cytoskeleton and vesicle mobility in astrocytes. Traffic 8:12–20.
Rock RS, Rice SE, Wels AL, Purcell TS, Spudich JA, Sweeny HL (2007) Myosin VI is a processive motor with a large step size. Proc Natl Acad Sci USA 98:13655–13659.
Rodriguez JJ, Mackie K, Pickel VM (2001) Ultrastructural localization of the CB1 cannabinoid receptor in mu-opioid receptor patches of the rat caudate putamen nucleus. J Neurosci 21:823–833.
Shumay E, Gavi S, Wang HY, Malbon CC (2004) Trafficking of β2-adrenergic receptors: insulin and β-agonists regulate internalization by distinct cytoskeletal pathways. J Cell Sci 117:593–600.
Simard M, Arcuino G, Takano T, Liu QS, Nedergaard M (2003) Signaling at the gliovascular interface. J Neurosci 23:9254–9262.
Stachelek SJ, Tuft RA, Lifschitz LM, Leonard DM, Farwell AP, Leonard JL (2001) Real-time visualization of processive myosin 5a-mediated vesicle movement in living astrocytes. J Biol Chem 276:35652–35659.
Stella N (2004) Cannabinoid signaling in glial cells. Glia 48:267–277.
Uchigashima M, Narushima M, Fukaya M, Katona I, Kano M, Watanabe M (2007) Subcellular arrangement of molecules for 2-arachidonoyl-glycerol-mediated retrograde signaling and its physiological contribution to synaptic modulation in the striatum. J Neurosci 27:3663–3676.
Venance L, Piomelli D, Glowinski J, Giaume C (1995) Inhibition by anandamide of gap junctions and intercellular calcium signalling in striatal astrocytes. Nature 376:590–594.
Verkhratsky A (2006) Glial calcium signaling in physiology and pathophysiology. Acta Pharmacol Sin 27:773–780.
Wilhelm A, Volknandt W, Langer D, Nolte C, Kettenmann H, Zimmermann H (2004) Localization of SNARE proteins and secretory organelle proteins in astrocytes *in vitro* and *in situ*. Neurosci Res 48:249–257.
Zhou M, Kimelberg HK (2000) Freshly isolated astrocytes from rat hippocampus show two distinct current patterns and different [K(+)](o) uptake capabilities. J Neurophysiol 84:2746–2757.

**Received 31 July 2009/6 November 2009; accepted 11 November 2009**
**Published as Immediate Publication 11 November 2009, doi 10.1042/AN20090040**